PATCH-BASED SENSOR PATTERN NOISE FOR CAMERA SOURCE IDENTIFICATION

Yue Tan, Bo Wang, Meijuan Zhao, Xiangwei Kong, and Ming Li

School of Information and Communication Engineering
Dalian University of Technology
Dalian, Liaoning, 116024, P. R. China
E-mail: {yue985,zhaomeijuan}mail.dlut.edu.cn, {bowang,kongxw,mli}dlut.edu.cn

ABSTRACT

Sensor pattern noise (SPN) has been proved to be an inherent fingerprint of a camera, and it has been broadly used in the fields of image authentication and camera source identification. However, the SPN extracted using current denoising algorithm always contains image content residual, which would significatively influence the accuracy of camera source identification. In this paper, a novel patch-based (PB) sensor pattern noise algorithm for camera source identification is proposed to solve this problem. Low-complexity patches of images are selected to construct local reference SPN, which contains least image content residual. The global reference SPN is constituted with the block-wised local SPN. Similarly for the test image, SPN is extracted from low-complexity region, and making correlation with corresponding local reference SPN. Our experiments on the Dresden database demonstrate that the proposed approach outperforms two sensor pattern noise estimation methods on the literatures as baseline.

***Index Terms*—** Sensor pattern noise, source camera identification, image complexity, patch-based sensor pattern noise.

1. INTRODUCTION

In last decade, digital image acquisition devices have become popular because of the much lower cost. As a result, the digital images are used to record events, testify incidents, and provide legally evidence for courtroom purposes. At the same time, there are more and more digital image processing techniques and photo editing software, which greatly reduce the integrity of digital images. As an important branch of passive digital image forensics, source camera identification focuses on the authentication of the originality of digital images. In recent years, various techniques have been proposed to solve the problem of source camera identification. These approaches can be categorized into two classes: Model-based and camera-based source identifications. A typical solution of model-based camera source identification is based on multi-dimensional statistical characteristic for classification. For example, Swaminathan *et al.* [1] proposed a method for source camera identification by the estimation of CFA pattern and interpolation kernel, which can gain an overall average accuracy of 90% for 19 camera brands. Kharrazi *et al.* [2] proposed 34 features which can be categorized into three types: Color features, image quality measurement (IQM), and high order wavelet characteristics (HOWS). A classifier based on these features can achieve an average accuracy of 88.02%. Recently, Xu and Shi used the uniform gray-scale invariant local binary patterns (LBP) [3] and received an average classification accuracy of 98.0%. The camera-based source identification focus on tracing a unique intrinsic fingerprint of a specific device. This work is mainly based on the sensor pattern noise. Lukas *et al.* first utilized the photo response non-uniformity noise of imaging sensors as a device fingerprint for camera-based source identification [4]. In [5], Hu *et al.* proposed an algorithm only comparing the large components of reference and test SPN. In [6], they proposed three schemes for combining information coming for three color channels that are an evolution of the large components technique presented in [5]. Later on, a series of improved algorithms were proposed in [7]-[9]. Most of these methods focus on estimating more accurate SPN and choosing a better correlation criterion.

In this paper, we propose a patch-based SPN method to identify the camera source. First of all, the image complexity is considered as an important factor that influences the accuracy of camera source identification. Then, a patch-based SPN method is proposed to generate a block-wised reference SPN. On the test phase, we select the test patch based on the image complexity, and calculate the correlation coefficient between the test patch with the corresponding block in reference SPN. Comparisons between the proposed method and two baselines from literatures verify the performance improvements of the proposed method. The rest of the paper is organized as follows. In Section 2, we introduce image complexity and present the proposed patch-based SPN method for camera source identification. In Section 3, experimental results demonstrate the efficiency of the proposed method. Finally, conclusions are drawn in Section 4.

2. PROPOSED METHOD

The image content residual is an inherent signal in SPN extraction, no matter what denoising algorithm adopted in the

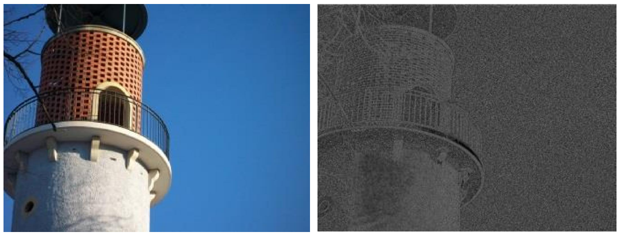

(a) (b)

Fig. 1. (a) An image taken by camera Kodak-M1063. (b) The SPN extracted from (a) by the method proposed in [4].

algorithm, as shown in Fig. 1. However, the residual intensity differs the accuracy of source camera identification. Previous works [10] have been proved that a cleaner SPN with less image content residual achieves a higher identification accuracy. Motivated by this factor, a novel patch-based SPN extraction method is proposed in this section, by quantitatively analyzing the image texture complexity.

2.1. Image complexity

Since image can be modeled as a region smooth Markov Distribution. Correlation can be found in neighborhood pixels. The difference between neighborhood pixels can approximately reflect the texture complexity of image. Considering an image I, $\mathbf{I}_{i,j}$ represents the value of pixel (i, j), and $\mathbf{I}_{i,j+1}$, $\mathbf{I}_{i+1,j}$ represent the values of horizontal and vertical neighborhood pixels of $\mathbf{I}_{i,j}$, respectively. Then, the horizontal and vertical differences can be defined as:

$$x = \mathbf{I}_n - \mathbf{I}_{n+1} \tag{1}$$

According to [10], the differences between neighborhood pixels can be modeled as a random Generalized Gaussian distribution (GGD) [11] variable with zero mean. The definition of GGD is given by:

$$\mathbf{p}_{\alpha,\beta}(x) = \frac{\beta}{2\alpha\Gamma(1/\beta)} exp(-(\frac{|x|}{\alpha})^2), \tag{2}$$

$$\alpha = \sigma\sqrt{\frac{\Gamma(1/\beta)}{\Gamma(3/\beta)}}, \sigma > 0, \tag{3}$$

where the Γ is the gamma function:

$$\Gamma(z) = \int_0^\infty e^{-t}t^{z-1}dt, z > 0. \tag{4}$$

Three parameters σ^2, α, and β in equation (2) represent variance, scale parameter, and shape parameter, respectively. These parameters can be rapidly estimated by the method in [12]. When the value of β drops, the shape of GGD probability density function become sharper. A smooth image means most of the difference values between neighborhood pixels will be around zero, namely a sharp GGD probability density function with a smaller value of β. On the contrary, a texture image implies a larger β. Therefore, there is a strong correlation between the shape parameter and the image texture complexity. In this paper, we define the complexity β_{hv} as the arithmetic average of the horizontal complexity β_h and the vertical complexity β_v , $\beta = (\beta_h + \beta_v)/2$. Fig. 2 (a) is the original image, and Fig. 2 (b) shows the β_{hv} values of each patch. The patches with the amount of texture will get a larger value of β_{hv}, while the smooth patches, such as that of sky only will obtain a smaller value of β_{hv}, as described before.

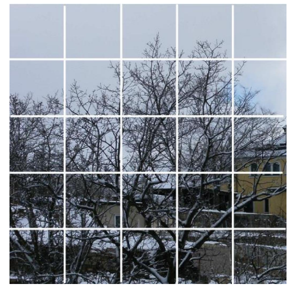

0.26	0.29	0.36	0.40	0.31
0.43	0.49	0.70	0.80	0.52
0.78	0.77	0.83	0.83	0.66
0.70	0.66	0.63	0.62	0.55
0.57	0.56	0.53	0.52	0.53

(a) (b)

Fig. 2. (a) An image taken by camera Kodak-M1063. (b) The image complexity of each patch.

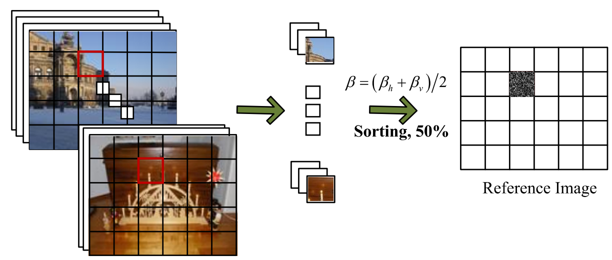

Fig. 3. The block diagram of patch-based SPN generation.

2.2. Patch-based SPN

Lukas *et al*. [4] proposed to use the average residual signals to construct the reference SPN. Residual signal $\mathbf{r}_i$ is obtained by $\mathbf{r}_i = \mathbf{I}_i - F(\mathbf{I}_i)$, where $\mathbf{I}_i$ is an original image and $F(\mathbf{I}_i)$ is the denoised image by a wavelet-based de-noising filter. Then, the reference SPN is given by:

$$K = \frac{\sum_{i=1}^{N} \mathbf{r}_i}{N} \tag{5}$$

where N is the number of images used to extract the SPN. We call this algorithm as Basic SPN in this paper.

Then, Goljian *et al*. [13] proposed a new SPN estimation technique, named the Maximum Likelihood Estimator (MLE) for camera source identification. The method of reference SPN generation is given by:

$$K = \frac{\sum_{i=1}^{N} \mathbf{r}_i\mathbf{I}_i}{\sum_{i=1}^{N} (\mathbf{I}_i)^2}. \tag{6}$$

Table 2. Accuracy of Basic SPN and proposed PBB SPN

Image size	Method	Casio-EX Z150	FujiFilm FinePixJ50	Kodak M1063	Nikon D200	Olympus mju	Panasonic DMC	Pentax OptioA40
256×256	Basic SPN	93%	88%	48%	86%	90%	94%	90%
	PBB SPN	92%	99%	85%	99%	88%	95%	90%
512×512	Basic SPN	98%	85%	91%	95%	93%	94%	95%
	PBB SPN	99%	100%	93%	99%	90%	98%	97%

Table 3. Accuracy of MLE SPN and proposed PBM SPN

Image size	Method	Casio-EX Z150	FujiFilm FinePixJ50	Kodak M1063	Nikon D200	Olympus mju	Panasonic DMC	Pentax OptioA40
256×256	MLE SPN	97%	97%	72%	93%	90%	98%	92%
	PBM SPN	89%	99%	77%	98%	90%	96%	87%
512×512	MLE SPN	99%	90%	95%	98%	93%	96%	98%
	PBM SPN	99%	99%	93%	99%	92%	100%	97%

In this paper, the image complexity is introduced to the processing of reference SPN generation. Assuming there are n images $\mathbf{I}_i (i = 1, 2, \dots, n)$ taken by camera c. First of all, each image is divided into several patches with a size of 128×128. Then, the complexity parameter β of each patch is calculated. According to the value of β, the patches in the same location are sorted in an ascend order. For the purpose of using the smooth image regions to generate the reference SPN, 50% of the patches with the minimum values of β are selected to construct local reference SPN. For a fair comparison, the basic SPN and MLE method mentioned above are respectively used as the method to extract the reference SPN from the selected smooth images. In the rest of paper, we call these two methods as PBB SPN and PBM SPN, respectively. Then, these local reference SPN patches are combined to obtain a large reference SPN. The block diagram of patch-based SPN generation is shown in Fig. 3. For the test image, we also divide the image into patches, and calculate the complexity parameter β of each patch. The patch with the smallest value is selected to extract residual noise. In the end, we calculate the correlation between the SPN of the selected patch and the reference SPN of corresponding region.

3. EXPERIMNETS

3.1. Experimental setting

In our experiments, a total of 1050 images from 7 cameras, which come from the Dresden Image Dataset [14], are considered. Table 1 demonstrates the details of the seven digital cameras which have been used in our experiments. For all experiments, the reference SPN is extracted from 50 images, and the test images is a set of 700 images, 100 images for each camera. For the comparison purpose, Basic SPN method [4] and MLE method [13] are employed as the baseline. In [4], the NCC is used to calculate the correlation. Different with that in [4], the Perk to Correlation Energy ratio (PCE) is used to evaluate the correlation in [13]. In order to conduct a fair comparison, we utilize the same correlation criterions of the PCE, which is given by:

Table 1. Details of the dataset used in experiments

Camera model	Resolution	Number
Casio-EX-Z150	3264×2448	150
FujiFilm-FinePixJ50	3264×2448	150
Kodak-M1063	3664×2748	150
Nikon-D200	3872×2592	150
Olympus-mju	3648×2736	150
Panasonic-DMC	3264×2736	150
Pentax-OptioA40	4000×3000	150

$$\begin{aligned} PCE(u) &= \frac{ncc(\mathbf{S}_{perk}, u)^2}{\frac{1}{mn-|N|}\sum_{s \notin N} ncc(s, u)^2} \\ &= \frac{\mathbf{r}_{xy}{}^2(0)}{\frac{1}{mn-|N|}\sum_{u \notin N} \mathbf{r}_{xy}{}^2(u)} \end{aligned} \quad (7)$$

where m and n refer to the size of the image, and for each fixed u, N is a small region surrounding the peak value of NCC, $\mathbf{S}_{perk}$, across all shifts $\mathbf{s}_1, \mathbf{s}_2$. The reference SPN is extracted by the PB method proposed in section 2.2. In this paper, we only consider the region on the upper left region, and the size is 128×12, 128×24. At the same time, for a test image, we attempt to find one image patch, which contains least

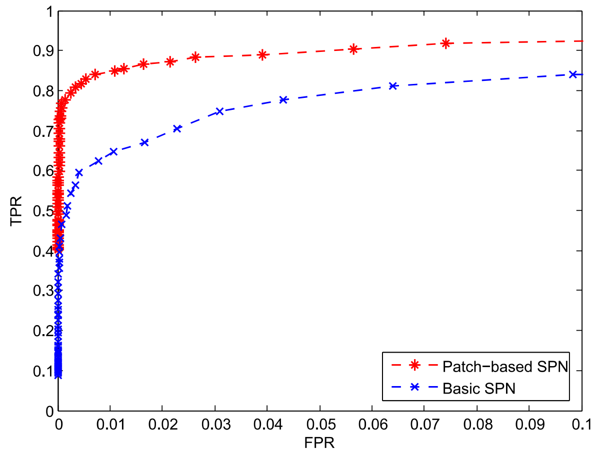

Fig. 4. Roc curves of Basic and PBB SPN for image size 256×256.

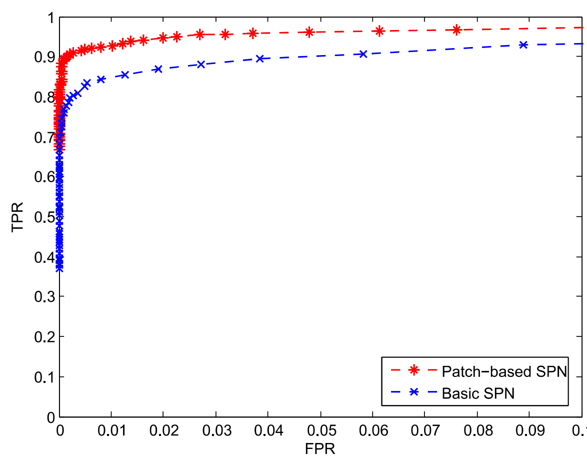

Fig. 5. Roc curves of Basic and PBB SPN for image size 512×512.

image texture in the same region as described above, and calculate the correlation with corresponding region in reference SPN. As for the size of patch to construct reference SPN is 128×128, in this paper, only two sizes of test image patches $(256 \times 256, 512 \times 512)$ have been considered to verify the performance of the proposed method.

3.2. Performance evaluation

Table 2 and Table 3 demonstrates the identification accuracies of the proposed methods PBB and PBM for each camera. We receive a better performance compared with the baseline proposed in [4] and [13]. From Table 2, we can see a significant improvement with an image size of 256×256 with an average increase up to 8% in accuracy. For the size of 512×512, the improvements reach 4%. Similar results can be found in Table 3. ROC curves have been also used in this paper to assess the performance of camera source identification as well as the accuracy. We plot the ROC curves for these four-groups comparisons, as shown in Fig. 4-7. More significant performance improvements of the proposed methods could be found

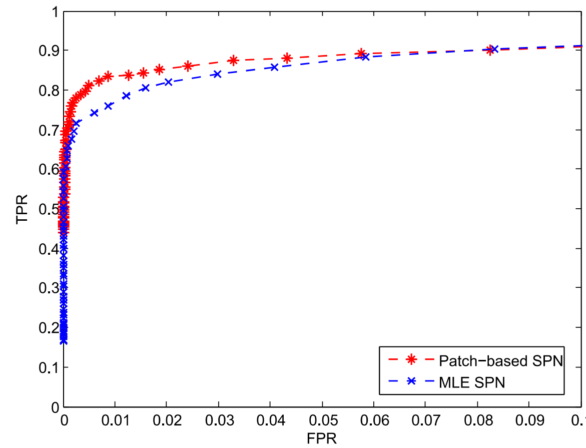

Fig. 6. Roc curves of MLE and PBM SPN for image size 256×256.

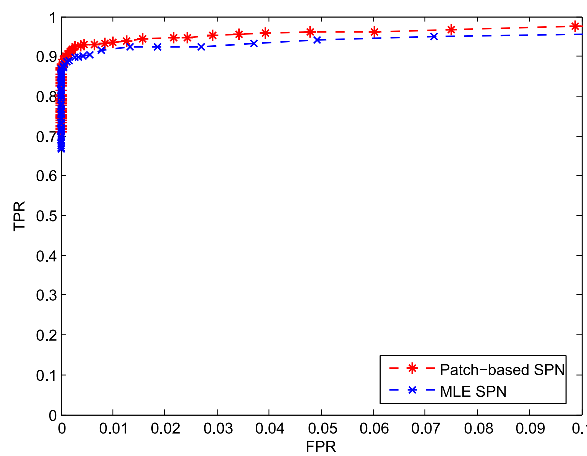

Fig. 7. Roc curves of MLE and PBM SPN for image size 512×512.

in these experimental results.

4. CONCLUSION

A patch-based (PB) sensor pattern noise method was proposed for camera source identification in this paper. Based on the observation that the SPN extracted from the smooth image regions has less image content residual, the parameters of image complexity were estimated for selecting the patches to construct the reference SPN and extract the test SPN. Experimental results demonstrated that the proposed approaches outperform two previously proposed sensor pattern noise estimation methods.

5. ACKNOWLEDGMENTS

This work is supported by the Open Fund of Artificial Intelligence Key Laboratory of Sichuan Province (Grant No. 2012RZ01), and also the Fundamental Research Funds for the Central Universities (Grant No. DUT13RC201, DUT14RC(3)103).

6. REFERENCES

[1] A. Swaminathan, M. Wu, and K. J. R. Liu, "Nonintrusive com-ponent forensics of visual sensors using output images," *IEEE Trans. Inf. Forensics Security*, vol. 2, no. 1, pp. 91-105, Feb. 2007.

[2] O. Celiktutan, B. Sankur, and I. Avcibas, "Blind identification of source cell-phone model," *IEEE Trans. Inf. Forensics Security*, vol. 3, no. 3, pp. 553-566, Sept. 2008.

[3] T. Ojala, M. Pietikainen, and T. Maenpaa, "Multiresolution gray-scale and rotation invariant texture classification with local binary patterns," *IEEE Trans. Pattern Analysis and Machine Intelligence*, vol. 24, no. 7, pp. 971-987, Aug. 2002.

[4] J. Fridrich, J. Luk$\acute{a}$š and M. Goljan, "Digital camera identifica-tion from sensor pattern noise," *IEEE Trans. Inf. Forensics Security*, vol. 1, no. 2, pp. 205-214, Jun. 2006.

[5] B. Yu, Y. Hu, and C. Jian, "Source camera identification using large components of sensor pattern noise, *in Proc. International Conference on Computer Science and its Applications*, pp. 1-5, Dec. 2009.

[6] Y. Hu, C.-T. Li, and C. Jian, "Building fingerprints with infor-mation from three color bands for source camera identification," in *Proc. ACM Workshop on Multimedia in Forensics, Security and Intelligence*, New York, pp. 111-116, Oct. 2010.

[7] Chang-Tsun Li, "Source camera identification using enhanced sensor pattern noise," *IEEE Trans. Inform. Forensics Security*, vol. 5, no. 2, pp. 280-287, Jun. 2010.

[8] J. Fridrich, *Sensor Defects in Digital Image Forensic*. Springer New York, pp. 179-218, 2013.

[9] W. Baoji and Z. Tao, "Universal blind detection based on multiple classifiers fusion and image complesity," *Journal of computer Applications*, vol. 34, no. 1, pp. 113-118, Jun. 2014.

[10] G. Wu, X. Kang, and K. J. R. Liu, "A context adaptive predictor of sensor pattern noise for camera source identification," in *Proc. IEEE International Conference on Image Processing*, pp. 237-240, 2012.

[11] M. Hongpi, C. S. Tong, S. K. Choy, "A fast and effective model for wavelet subband histograms and its applications in texture image retreval," *IEEE Trans.* on Image Processing, vol. 15, no. 10, pp. 3078-3088, Jun. 2006.

[12] W. Taiyue, L. Zhiming, "A fast parameter estimation of generalized gaussion distribution," *Chinese Journal of Engineering Geophysics*, vol. 3, no. 3, pp. 172-175, Jun. 2006.

[13] M. Goljan, T. Filler, J. Fridrich, "Large scale test of sensor Fingerprint camera source identification," in Proc. *SPIE* Electronic Media Forensics and Security XI, San Jose, vol. 7254, pp. 0I 01-0I 12, Jun. 2009.

[14] T. Gloe and R. Bohme, "The 'Dresden Image Database' for benchmarking digital image forensics," in *Proc. ACM Symposium on Applied Computing*, Sierre, Switzerland, vol. 3, no. 2-4, 2010.